The Astrophysical Journal Letters, 728:L32 (5pp), 2011 February 20 doi:10.1088/2041-8205/728/2/L32

MEASUREMENTS OF ISOTOPE EFFECTS IN THE PHOTOIONIZATION OF N_2 AND IMPLICATIONS FOR TITAN'S ATMOSPHERE

Philip Croteau[1], John B. Randazzo[1], Oleg Kostko[2], Musahid Ahmed[2], Mao-Chang Liang[3,4], Yuk L. Yung[5], and Kristie A. Boering[1,6]

[1] Department of Chemistry, University of California, Berkeley, CA 94720, USA
[2] Chemical Sciences Division, Lawrence Berkeley National Laboratory, Berkeley, CA 94720, USA
[3] Research Center for Environmental Changes and Institute of Astronomy and Astrophysics, Academia Sinica, Taipei 115, Taiwan
[4] Graduate Institute of Astronomy, National Central University, Jhongli, Taiwan
[5] Division of Geological and Planetary Sciences, California Institute of Technology, Pasadena, CA 91125, USA
[6] Department of Earth and Planetary Science, University of California, Berkeley, CA 94720, USA; boering@berkeley.edu
Received 2010 June 18; accepted 2010 December 28; published 2011 January 28

ABSTRACT

Isotope effects in the non-dissociative photoionization of molecular nitrogen ($N_2 + h\nu \rightarrow N_2^+ + e^-$) may play a role in determining the relative abundances of isotopic species containing nitrogen in interstellar clouds and planetary atmospheres but have not been previously measured. Measurements of the photoionization efficiency spectra of $^{14}N_2$, $^{15}N^{14}N$, and $^{15}N_2$ from 15.5 to 18.9 eV (65.6–80.0 nm) using the Advanced Light Source at Lawrence Berkeley National Laboratory show large differences in peak energies and intensities, with the ratio of the energy-dependent photoionization cross sections, $\sigma(^{14}N_2)/\sigma(^{15}N^{14}N)$, ranging from 0.4 to 3.5. Convolving the cross sections with the solar flux and integrating over the energies measured, the ratios of photoionization rate coefficients are $J(^{15}N^{14}N)/J(^{14}N_2) = 1.00 \pm 0.02$ and $J(^{15}N_2)/J(^{14}N_2) = 1.00 \pm 0.02$, suggesting that isotopic fractionation between N_2 and N_2^+ should be small under such conditions. In contrast, in a one-dimensional model of Titan's atmosphere, isotopic self-shielding of $^{14}N_2$ leads to values of $J(^{15}N^{14}N)/J(^{14}N_2)$ as large as ~1.17, larger than under optically thin conditions but still much smaller than values as high as ~29 predicted for N_2 photodissociation. Since modeled photodissociation isotope effects overpredict the $HC^{15}N/HC^{14}N$ ratio in Titan's atmosphere, and since both N atoms and N_2^+ ions may ultimately lead to the formation of HCN, estimates of the potential of including N_2 photoionization to contribute to a more quantitative explanation of $^{15}N/^{14}N$ for HCN in Titan's atmosphere are explored.

Key words: astrochemistry – ISM: clouds – molecular processes – planets and satellites: atmospheres – planets and satellites: composition – planets and satellites: individual (Titan)

1. INTRODUCTION

Isotopic substitution often alters the chemical and physical properties of atoms and molecules, resulting in, for example, differences in absorption spectra, reaction rates, and atmospheric escape velocities. Because such isotope effects can lead to measurable changes in the relative abundances of the isotopologues of molecules in planetary atmospheres and interstellar molecular clouds, measurements of the isotopic compositions of various species can be used to interpret chemical and physical histories and/or chemical reaction pathways in these environments provided all relevant isotope effects are known. In particular, isotope effects in the non-dissociative photoionization of molecular nitrogen

$$N_2 + h\nu \rightarrow N_2^+ + e^- \qquad \text{(R1)}$$

have not been measured previously, despite their potential importance in a variety of environments, including interstellar molecular clouds (e.g., Trevia & Herbst 2000), the solar nebula (e.g., Bockelee-Morvan et al. 2008), and planetary atmospheres on Earth (e.g., Aikin 2001; Kaye 1987), Mars (e.g., McElroy et al. 1976; Fox & Hać 1997), and Saturn's moon, Titan (e.g., Wilson & Atreya 2004; Waite et al. 2007; Imanaka & Smith 2007, 2009, 2010). For Titan, quantification of possible isotope effects in Equation (R1) may lead to a better understanding of the chemical processes currently occurring in Titan's atmosphere that produce pre-biotic organic compounds such as benzene and aerosols (Wilson & Atreya 2004; Waite et al. 2007; Imanaka & Smith 2007, 2009, 2010) and of the origin and long-term evolution of its unusual and puzzlingly dense N_2 atmosphere (e.g., Liang et al. 2007a). For Earth, Equation (R1) may lead to enrichments or depletions in the isotope ratios of atmospheric trace species, such as NO, which may be useful as a tracer of stratospheric and thermospheric air masses in the mesosphere, and, hence, on atmospheric circulation in these regions (e.g., Aikin 2001). For Mars, the evolution of the martian atmosphere on a billion-year timescale may be better constrained by quantifying potential isotope effects in Equation (R1) that may lead to differences in the escape velocities of ^{15}N versus ^{14}N due to dissociative recombination of N_2^+ in Mars' upper atmosphere (e.g., McElroy et al. 1976; Fox & Hać 1997), similar to issues on Titan.

Here, we present measurements of the photoionization efficiency (PIE) spectra of $^{14}N_2$, $^{15}N^{14}N$, and $^{15}N_2$ using vacuum ultraviolet (VUV) synchrotron radiation from the Advanced Light Source (ALS) at Lawrence Berkeley National Laboratory from 15.5 eV to 18.9 eV. The experimental results for the isotope-specific photoionization cross sections are then used as input to a photochemical model of Titan's atmosphere to determine the ratios of photoionization rates and rate coefficients for $^{14}N_2$ and $^{15}N^{14}N$ relative to those for other processes, such as N_2 photodissociation, which are known to affect on the isotopic compositions of N_2 and HCN (e.g., Liang et al. 2007a).

2. PHOTOIONIZATION EFFICIENCY SPECTRA

A molecular beam apparatus coupled to the Chemical Dynamics Beamline (CDB) at the ALS (Nicolas et al. 2006; Kostko

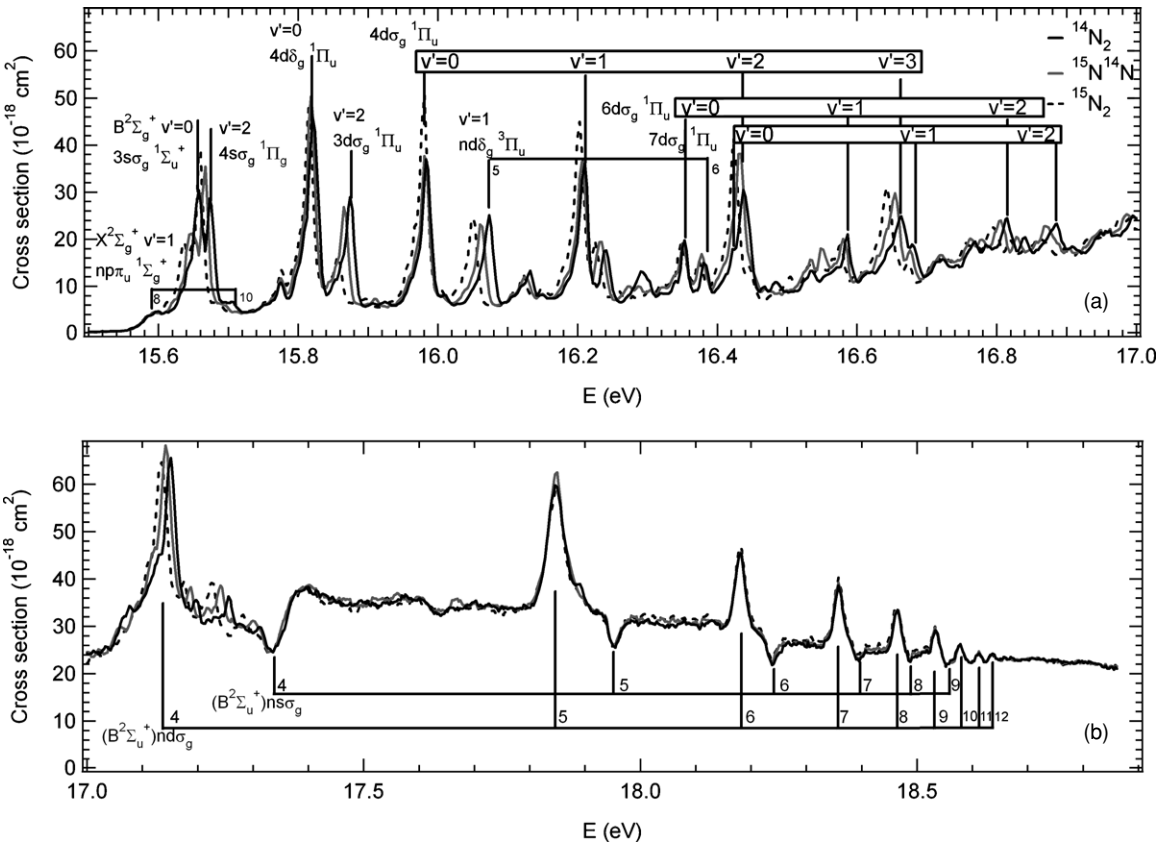

Figure 1. Photoionization efficiency spectra for $^{14}N_2$ (black solid lines), $^{15}N^{14}N$ (gray solid lines), and $^{15}N_2$ (black dashed lines) for (a) 15.5–17.0 eV and (b) 17.0–18.9 eV.

et al. 2008) was used to determine the relative photoionization cross sections as a function of energy for the three isotopologues of N_2. A beam of N_2 was formed by flowing an approximately 1:1:1 mixture of $^{14}N_2$ (Airgas, 99.999% purity N_2), $^{15}N^{14}N$ (Icon Services, 99%), and $^{15}N_2$ (Icon Services, 98%) into the source chamber of the apparatus using three calibrated mass-flow controllers (MKS 1179, 20 sccm full range; Andover, MA), each set to 2.5 sccm. This mixture then underwent supersonic expansion to form a molecular beam. Although the temperature of the beam was not measured directly, experiments done under similar conditions have yielded N_2 translational and rotational temperatures of $\leqslant$50 K (e.g., Aoiz et al. 1999; Mori et al. 2005), and little vibrational excitation is expected under these conditions; thus the N_2 beam was translationally, rotationally, and vibrationally cold. The beam was then crossed at 90° with monochromated VUV light from the synchrotron with a bandwidth of ~6.5 meV FWHM (~0.03 nm FWHM).

The resulting N_2^+ ions were then accelerated with Wiley–McLaren ion optics and separated by mass-to-charge ratio (m/z) in a reflectron time-of-flight mass spectrometer, and the time-dependent signal from a microchannel plate detector was collected with a multichannel-scaler card and then integrated with a PC. The peaks corresponding to $^{14}N_2^+$, $^{15}N^{14}N^+$, and $^{15}N_2^+$ were each integrated for each 3 meV energy step and then normalized by the photon flux, which was measured using an NIST-calibrated Si-photodiode. An additional normalization of the isotopologue photoionization signals was then performed—both to reduce the error associated with the 1% full-scale accuracy of the mass-flow controllers (which itself would yield a 10% uncertainty in the isotopologue mixing ratios at the gas nozzle) and to correct for any center line enrichment in the heavier isotopologues which may have occurred in the molecular beam (e.g., McLean & Sawyer 1974)—by doing the following: because there should be no isotope effects in direct photoionization to a continuum, the average and standard deviation for the ratios of the isotopologue signals in these relatively featureless regions of the spectra were used to calculate more accurate mixing ratios of the isotopologues in the interaction region between the molecular beam and the photon beam. This procedure yielded values of 0.339 ± 0.002, 0.321 ± 0.002, and 0.340 ± 0.002 for $^{14}N_2$, $^{15}N^{14}N$, and $^{15}N_2$, respectively. The relative photoionization intensities for each isotopologue were then normalized by these experimentally determined mixing ratios. Finally, the relative photoionization intensities were converted to cross sections using previous measurements of the photoionization cross sections for $^{14}N_2$ (Samson et al. 1977; Itikawa et al. 1986). Additional experimental details will be published elsewhere.

Figure 1 shows the PIE spectrum for each isotopologue from 15.5 to 18.9 eV along with peak assignments. The major features in the photoionization spectra are autoionizing Rydberg states converging to vibrational levels of the second ($A^2\Pi_u$) and third ($B^2\Sigma_u^+$) ionized states of N_2 which shift in energy and/or intensity upon isotopic substitution. Based on higher resolution PIE spectra available for $^{14}N_2$ (e.g., Dehmer et al. 1984; Sommavilla et al. 2002), some rotational lines for peaks near the photoionization threshold (i.e., for energies $\leqslant$15.8 eV in Figure 1) are not resolvable with the 6.5 meV resolution of this experiment, while peaks above 15.8 eV appear to be fully resolved in this study.

Figure 2 shows the ratio of the photoionization cross sections for (a) $^{14}N_2/^{15}N^{14}N$ and (b) $^{14}N_2/^{15}N_2$; the light/heavy ratios

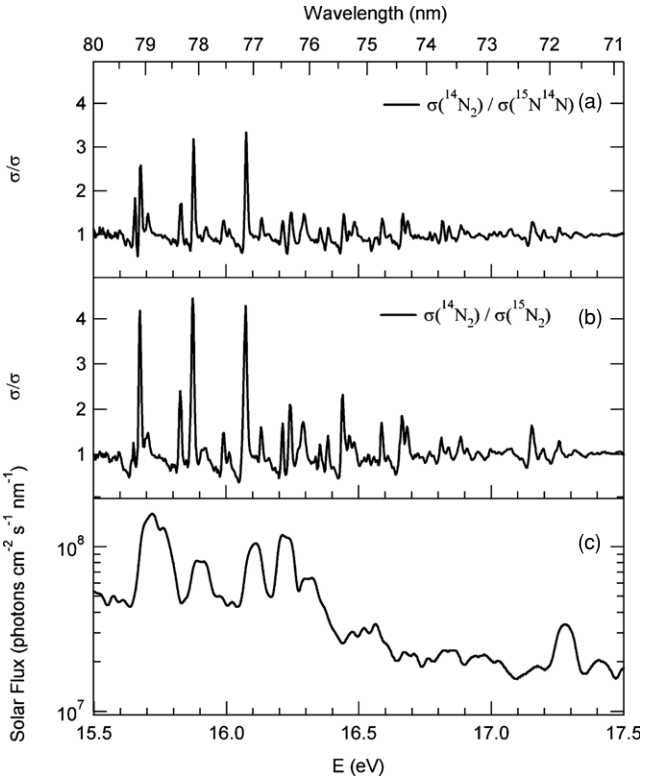

Figure 2. Ratios of photoionization cross sections for (a) $^{14}N_2/^{15}N^{14}N$ and (b) $^{14}N_2/^{15}N_2$ over the range 15.5–17.5 eV (note that the isotope shifts are negligible between 17.5 and 18.9 eV and are not shown here). For comparison, the solar spectrum from Woods et al. (1998) with a resolution of 0.2 nm (∼40 meV) and scaled at 1 AU is shown over the same energy range.

can exceed a factor of four for the ∼6.5 meV bandwidth of the experiment at several different energies. Isotopic fractionation of N_2 (as well as of species that may react with the resulting N_2^+ or with the two nitrogen atoms after dissociative electron recombination of N_2^+) in a planetary atmosphere, however, depends not just on the ratios of cross sections at one particular energy, however, but on the isotope effects convolved with the radiation intensity and integrated over a range of energies—in other words, isotopic fractionation will depend on the ratios of the photoionization rate coefficients, J, for the different isotopologues given by Equation (1):

$$J = \int_{E_i}^{E_f} \sigma(E) I(E) dE, \quad (1)$$

where $\sigma(E)$ is the photoionization cross section, $I(E)$ is the radiation intensity, and the integral is over the energies E_i to E_f. Under "white light" irradiation and optically thin conditions, the ratios of the J-values over the entire experimental energy range are $J(^{15}N^{14}N)/J(^{14}N_2) = 1.01 \pm 0.02$ and $J(^{15}N_2)/J(^{14}N_2) = 1.00 \pm 0.02$. Using the solar spectrum shown in Figure 2(c) for $I(E)$ (Woods et al. 1998; Ribas et al. 2005) yields 1.00 ± 0.02 for $J(^{15}N^{14}N)/J(^{14}N_2)$ and 1.00 ± 0.02 for $J(^{15}N_2)/J(^{14}N_2)$. Thus, to zeroth order in an optically thin planetary atmosphere under solar irradiation in which no species alter the actinic flux, isotopic fractionation of N_2 via Equation (R1) is predicted to be small at these energies.

3. PHOTOCHEMICAL MODEL

In the dense, N_2-rich atmosphere of Titan, however, isotopic self-shielding may occur for which radiation propagating from the top of the atmosphere to lower altitudes is attenuated much more rapidly by the common isotopologue $^{14}N_2$ than by the rare isotopologue $^{15}N^{14}N$; hence, at some altitude, the atmosphere becomes optically thick in the particular energies absorbed by $^{14}N_2$ but allows radiation at energies that photoionize $^{15}N^{14}N$ to continue to propagate. In principle, this process may lead to an increasingly larger photoionization rate coefficient for $^{15}N^{14}N$ relative to $^{14}N_2$ with decreasing altitude, as has been calculated recently by Liang et al. (2007a) for N_2 photodissociation

$$N_2 + h\nu \rightarrow 2N, \quad (R2)$$

using isotope-specific photodissociation cross sections calculated theoretically by the diabatic coupled-channel Schrödinger equation model (Liu et al. 2008).

To test the extent to which isotopic self-shielding due to N_2 photoionization could significantly affect the relative photoionization rates of $^{14}N_2$ versus $^{15}N^{14}N$, and hence might play a role in determining the isotopic composition of N_2 and nitrogen-containing photochemical products in Titan's atmosphere, the measured cross sections for photoionization of $^{14}N_2$ and $^{15}N^{14}N$ were included in a one-dimensional (1D) photochemical model of Titan's atmosphere (Yung et al. 1984; Liang et al. 2007a, 2007b). In Liang et al. (2007a), a diurnally averaged 1D model was used to calculate the vertical profiles of H, H_2, C_1–C_2, N, N_2, CN, HCN, NH, and isotopic compounds of nitrogen by solving the mass continuity equations for these species and using the vertical eddy mixing coefficients, neutral species reaction schemes, temperature profile, transport, and physicochemical molecular processes as in Liang et al. (2007b). The solar flux used in Liang et al. (2007a) was that of Woods et al. (1998) with an FWHM of 0.2 nm (shown here in Figure 2(c)); full resolution calculations using a semi-empirical high-resolution model of solar output on the order 0.0001 nm FWHM showed that the calculated $[HC^{14}N]/[HC^{15}N]$ ratios changed by less than 2% when the 0.0001 nm FWHM resolution solar flux was used. Finally, we note that the N_2 vertical profile modeled by Liang et al. (2007a) was consistent with that derived from observations (e.g., Waite et al. 2007; Liang et al. 2007b). For this study, we used the same model to calculate the relative photoionization rate coefficients for $^{14}N_2$ versus $^{15}N^{14}N$ as a function of altitude to see how these compare with the predicted large isotopic self-shielding effects due to N_2 photodissociation.

The model results are given in Figure 3 and show that—due to isotopic self-shielding—the J-value for $^{15}N^{14}N$ photoionization is larger than that for $^{14}N_2$ in Titan's atmosphere and significantly larger than the ratio of 1.00 ± 0.02 predicted simply using Equation (1) with the solar flux at the top of the atmosphere. For example, at 1100 km, where the rate of N_2 photoionization is at its maximum (solid lines in the left panel of Figure 3), the ratio of photoionization J-values, $J(^{15}N^{14}N)/J(^{14}N_2)$, is 1.08 (solid lines in the right panel of Figure 3; note that in the right panel, the ratios of J-values for photoionization are plotted as $(J(^{15}N^{14}N)/J(^{14}N_2)–1) \times 100$), which is the fractionation constant in percent, or 8% in this instance). At 900 km, where the photoionization rates are ∼30% of their maximum, the ratio $J(^{15}N^{14}N)/J(^{14}N_2)$ reaches a value as high as 1.17, corresponding to a fractionation constant of 17%. (Note that the higher value of the ratio of ∼1.20 at 600 km corresponds to where the photoionization rate is near zero.) For comparison, the same model yields values for the ratio $J(^{15}N^{14}N)/J(^{14}N_2)$ for N_2 photodissociation as high as a 29 (corresponding to a fractionation constant of 2800%; see the right panel of Figure 3). Thus, while isotopic self-shielding due to N_2 photoionization is predicted to

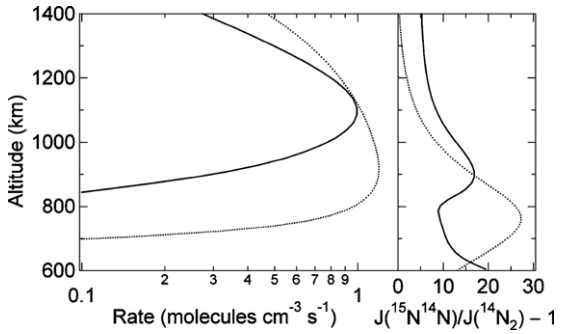

Figure 3. Left panel: model-calculated rates for N_2 photoionization (solid line) and N_2 photodissociation (dotted line) for $^{14}N_2$ in Titan's atmosphere, using the same N_2 profile as in Liang et al. (2007a). Right panel: fractionation constants ($J(^{15}N^{14}N)/J(^{14}N_2) - 1$)) for the model-calculated isotope-specific rate coefficients, J, for photoionization (solid line) and photodissociation (dotted line) showing the effects of isotopic self-shielding by $^{14}N_2$. The values for the photoionization fractionation constant in the right panel have been multiplied by a factor of 100 (to yield the photoionization fractionation constant in percent).

occur in Titan's atmosphere, the largest fractionation constant for photoionization from this study is predicted to be ∼160 times smaller than that for photodissociation.

4. DISCUSSION

The isotope-specific photoionization cross sections for N_2 reported here are a good starting point for astrochemical applications and suggest that isotopic self-shielding may be important enough to include when considering the isotopic fractionation of molecular nitrogen and its subsequent photoproducts in various environments. The molecular beam conditions in the experiment of ∼50 K are appropriate for some of these environments, while changes in the absolute and relative photoionization cross sections with temperature due to changes in state populations and/or Doppler widths may need to be taken into account in models of environments at higher temperatures. For example, using the theoretical isotope-specific photodissociation cross sections from Liang et al. (2007a), we found that predictions of the magnitude of isotopic self-shielding in a Titan-like atmosphere held at constant temperatures of 100, 150, and 200 K decreased with increasing temperature, with the ratio of J-values for $^{15}N^{14}N$ versus $^{14}N_2$ decreasing from a value of ∼29 to ∼25 over this temperature range. Such an inverse temperature dependence for isotopic shielding effects has also been found by Visser et al. (2009) in models of isotopic self-shielding in CO photodissociation. Thus, the prediction of the magnitude of isotopic self-shielding in Titan's atmosphere using our experimental PIE results directly without taking the effects of temperature changes on the PIE spectra into account, as we have done in the preliminary model results given here, is likely to represent an upper limit. In contrast, the fact that our experimental resolution of 6.5 meV does not resolve rotational lines in several of the peaks near threshold (below energies of ∼16 eV) means that the model results presented here may represent a lower limit for isotopic self-shielding in N_2 photoionization: as Visser et al. (2009) have shown, a narrowing of peaks will usually result in more isotopic selectivity and thus more shielding. The extent to which this limit may be significant can be addressed in future experimental studies by making higher resolution isotope-specific measurements focused on the 15.6 and 15.8 eV regions of the spectra.

Despite the current quantitative limitations noted above which can be addressed in future studies, we outline here several potential applications of such isotope-specific data to Titan's atmosphere that the new laboratory measurements suggest are worth considering. Observations of the $^{15}N/^{14}N$ ratio of HCN and N_2 in Titan's atmosphere—including measurements from the CIRS and INMS instruments on the *Cassini* orbiter (Vinatier et al. 2007; Waite et al. 2005), the GCMS instrument on the Huygens probe (Niemann et al. 2005), and ground-based observations of $^{15}N/^{14}N$ of HCN (Gurwell 2004; Marten et al. 2002)—have shown that the ratio for HCN is larger by a factor of two to four than that for the parent N_2. Since N atoms formed by the photodissociation of N_2 can react with various hydrocarbons to form HCN, Liang et al. (2007a) suggested that the large isotopic self-shielding effects they calculated for N_2 photodissociation would result in a ^{15}N-enriched N atom pool which would then form ^{15}N-enriched HCN relative to the parent N_2. However, when they incorporated isotope effects in N_2 photodissociation into their model, the resulting $^{15}N/^{14}N$ ratio of HCN was too large; they thus suggested that other processes were still required to explain the observations, which might include a flux of ^{15}N-depleted N atoms produced by ion/electron impact from the top of the atmosphere.

The experimental and modeling results presented here suggest that potential additional pathways to forming HCN which may affect its isotopic composition should be examined. HCN can potentially be formed starting with N_2^+ ions via two mechanisms. The first is via dissociative recombination with electrons ($N_2^+ + e^- \rightarrow 2N$), forming N atoms which can then react with photochemical products of methane to form HCN, just as the N atoms from the direct photodissociation of N_2 do (e.g., Yung et al. 1984; Vuitton et al. 2007; Krasnopolsky 2009). Given the rate coefficient for dissociative recombination and the N_2^+ and electron densities in Vuitton et al. (2007), however, the maximum rate of production of N atoms via this pathway is at 1100 km and is about 1000 times slower than that produced by direct N_2 photodissociation at this altitude and would therefore not be expected to alone account for the overprediction by Liang et al. (2007a) of the isotopic enrichment in HCN due to N_2 photodissociation, although it would change it in the correct direction. The second mechanism to produce HCN that is isotopically lighter than that produced via N_2 photodissociation could be through ion–molecule reactions of N_2^+ with C_2H_2 and C_2H_4, which are present in significant concentrations in Titan's upper atmosphere (Vuitton et al. 2007). However, the laboratory data on rate coefficients and branching ratios for these pathways to HCN remain ambiguous as to how fast such reactions occur or whether they occur at all (e.g., Anicich & McEwan 1997; McEwan & Anicich 2007). An upper limit to the HCN production rate at 1100 km from $N_2^+ + C_2H_4$ is ∼0.03 molec cm^{-3} s^{-1} while that for $N_2^+ + C_2H_2$ is $\sim 5 \times 10^{-5}$ molec cm^{-3} s^{-1}, based on rate coefficients and branching ratios from Anicich & McEwan (1997), mixing ratio measurements from Vuitton et al. (2007), and the mean day–night pressure at 1100 km from Vinatier et al. (2007). The largest rate (for $N_2^+ + C_2H_4$) is ∼100 times lower than HCN production from the $N + CH_3$ reaction (3 molec cm^{-3} s^{-1}), which is the major production pathway for HCN at this altitude, where N is derived primarily from N_2 photodissociation.

Thus, based on the estimates above, isotope effects in the non-dissociative photoionization of N_2 are not expected to play a large role in determining the isotopic composition of HCN near 1100 km, although careful modeling work that includes isotope effects in ion–molecule chemistry is still warranted. In addition, it may also be necessary to include isotope effects

in the dissociative photoionization of N_2 in such models; these isotope effects have not yet been measured directly, but electron impact studies suggest that dissociative photoionization proceeds through predissociative states and should therefore exhibit significant isotopic shifts in energies and intensities (Govers et al. 1975 and references therein).

Finally, we note that the very large differences in isotopic fractionation arising from photoionization versus photodissociation of N_2 suggested by the isotope-specific *J*-values modeled here for Titan's atmosphere might potentially provide a means of determining the relative importance of chemical pathways for the production of organic compounds and aerosol (or tholins) on Titan in future missions. *Cassini* measurements reveal two distinct mechanisms for organic synthesis (see recent reviews by Waite et al. 2009 and Cravens et al. 2009): a new synthesis process that is largely driven by ion chemistry occurs in the ionosphere of Titan, above 1000 km, in addition to the neutral chemistry that occurs lower in the atmosphere (Yung et al. 1984). Figure 3 shows that the isotopic fractionations by photoionization and photodissociation of N_2—the starting points of these two synthetic processes—are distinct. Hence, measurements of the nitrogen isotopic composition of organic compounds and tholins, when this becomes feasible, could potentially offer a means to discriminate between their origins.

In summary, while isotopic fractionation of nitrogen in the atmosphere of Titan due to neutral chemistry has been modeled by Liang et al. (2007a), a similar study of isotopic fractionation of nitrogen due to ion chemistry has not been done. The experimental and modeling results presented here provide a strong motivation to pursue such a modeling study, to measure the near-threshold photoionization features for $^{14}N_2$ and $^{15}N^{14}N$ at higher resolution, and to measure isotope effects in the dissociative photoionization of N_2. More generally, these first measurements of isotope effects in the non-dissociative photoionization of N_2 demonstrate that this reaction could in principle play a previously ignored and potentially important role in isotopic fractionation in planetary atmospheres and other environments in which N_2 and VUV radiation are present.

We gratefully acknowledge support from NASA Planetary Atmospheres grant NNX08AE69G to UC Berkeley and a Dreyfus Teacher-Scholar Award for K.A.B.; from the Director, Office of Energy Research, Office of Basic Energy Sciences, Chemical Sciences Division of the U.S. Department of Energy under contract no. DE-AC02-05CH11231 for O.K., M.A., and the ALS; from NSC grant 98-2111-M-001-014-MY3 to Academia Sinica for M.-C.L.; and NASA grant NX09AB72G to the California Institute of Technology for Y.L.Y.

REFERENCES

Aikin, A. C. 2001, Phys. Chem. Earth Part C, Sol.-Terr. Planet Sci., 26, 527
Anicich, V. G., & McEwan, M. J. 1997, Planet. Space Sci., 45, 897
Aoiz, F. J., et al. 1999, J. Phys. Chem. A, 103, 823
Bockelee-Morvan, D., et al. 2008, ApJ, 679, L49
Cravens, T. E., Yelle, R. V., Wahlund, J. E., Shemansky, D. E., & Nagy, A. F. 2009, in Titan from Cassini-Huygens, ed. R. H. Brown, J. P. Lebreton, & J. H. Waite (New York: Springer), 259
Dehmer, P. M., Miller, P. J., & Chupka, W. A. 1984, J. Chem. Phys., 80, 1030
Fox, J. L., & Hać, A. 1997, J. Geophys. Res., 102, 9191
Govers, T. R., van de Runstraat, C. A., & de Heer, F. J. 1975, Chem. Phys., 9, 285
Gurwell, M. A. 2004, ApJ, 616, L7
Imanaka, H., & Smith, M. A. 2007, Geophys. Res. Lett., 34, L02204
Imanaka, H., & Smith, M. A. 2009, J. Phys. Chem. A, 113, 11187
Imanaka, H., & Smith, M. A. 2010, Proc. Natl Acad. Sci. USA, 107, 12423
Itikawa, Y., et al. 1986, J. Phys. Chem. Ref. Data, 15, 985
Kaye, J. A. 1987, Rev. Geophys., 25, 1609
Kostko, O., Belau, L., Wilson, K. R., & Ahmed, M. 2008, J. Phys. Chem. A, 112, 9555
Krasnopolsky, V. A. 2009, Icarus, 201, 226
Liang, M. C., Heays, A. N., Lewis, B. R., Gibson, S. T., & Yung, Y. L. 2007a, ApJ, 664, L115
Liang, M. C., Yuk, Y. L., & Shemansky, D. E. 2007b, ApJ, 661, L199
Liu, X., et al. 2008, J. Geophys. Res., 113, A02304
Marten, A., Hidayat, T., Biraud, Y., & Moreno, R. 2002, Icarus, 158, 532
McElroy, M. B., Yung, Y. L., & Nier, A. O. 1976, Science, 194, 70
McEwan, M. J., & Anicich, V. G. 2007, Mass Spectrom. Rev., 26, 281
McLean, W. J., & Sawyer, R. F. 1974, Acta Astronaut., 1, 523
Mori, H., Niimi, T., Akiyama, I., & Tsuzuki, T. 2005, Phys. Fluids, 17, 117103
Nicolas, C., Shu, J. N., Peterka, D. S., Hochlaf, M., Poisson, L., Leone, S. R., & Ahmed, M. 2006, J. Am. Chem. Soc., 128, 220
Niemann, H. B., et al. 2005, Nature, 438, 779
Ribas, I., Guinan, E. F., Gudel, M., & Audard, M. 2005, ApJ, 622, 680
Samson, J. A. R., Haddad, G. N., & Gardner, J. L. 1977, J. Phys. B: At. Mol. Phys., 10, 1749
Sommavilla, M., Hollenstein, U., Greetham, G. M., & Merkt, F. 2002, J. Phys. B, 35, 3901
Trevia, R., & Herbst, E. 2000, MNRAS, 317, 563
Vinatier, S., Bézard, B., & Nixon, C. A. 2007, Icarus, 191, 712
Visser, R., van Dishoeck, E. F., & Black, J. H. 2009, A&A, 503, 323
Vuitton, V., Yelle, R. V., & McEwan, M. J. 2007, Icarus, 191, 722
Waite, J. H., Young, D. T., Cravens, T. E., Coates, A. J., Crary, F. J., Magee, B., & Westlake, J. 2007, Science, 316, 870
Waite, J. H., Young, D. T., Westlake, J. H., Lunine, J. I., McKay, C. P., & Lewis, W. S. 2009, in Titan from Cassini-Huygens, ed. R. H. Brown, J. P. Lebreton, & J. H. Waite (New York: Springer), 214
Waite, J. H., et al. 2005, Science, 308, 982
Wilson, E. H., & Atreya, S. K. 2004, J. Geophys. Res., 109, E06002
Woods, T. N., Rottman, G. J., Bailey, S. M., Solomon, S. C., & Worden, J. R. 1998, Sol. Phys., 177, 133
Yung, Y. L., Allen, M., & Pinto, J. P. 1984, ApJS, 55, 465